Magnetic Structure of Cr in Exchange Coupled Fe/Cr(001) Superlattices

A. Schreyer,[1] C. F. Majkrzak,[2] Th. Zeidler,[1] T. Schmitte,[1] P. Bödeker,[1] K. Theis-Bröhl,[1] A. Abromeit,[1]
J. A. Dura,[2] and T. Watanabe[2]
[1]*Experimentalphysik (Festkörperphysik), Ruhr-Universität Bochum, 44780 Bochum, Germany*
[2]*National Institute of Standards and Technology, Gaithersburg, Maryland 20899*
(Received 20 February 1997)

We demonstrate how the noncollinear exchange coupling between the Fe layers in Fe/Cr(001) superlattices is caused by a frustrated spiral modulation of the Cr moments not observed in bulk. The noncollinear coupling vanishes above the Néel temperature of this commensurate antiferromagnetic Cr order. This clarifies the essential contribution of Cr ordering to the coupling in the regime of smallest thicknesses where no incommensurate Cr spin density wave can form. For larger Cr thicknesses we observe a predicted incommensurate to commensurate transition with temperature. [S0031-9007(97)04817-5]

PACS numbers: 75.70.Cn, 75.25.+z, 75.30.Fv

The oscillatory exchange coupling between ferromagnetic (FM) layers over a non-FM interlayer [1], the related giant magnetoresistance effect [2], and the biquadratic or noncollinear (NC) exchange coupling between FM layers [3,4] were important recent discoveries in the field of thin film magnetism [5]. Fe/Cr(001) layered structures played the key role in these findings. Since Cr is antiferromagnetic (AF) in bulk [6], it is of fundamental importance to understand the role of the Cr magnetism in this model system.

After the discovery of the long range period of the exchange coupling in Fe/Cr(001) as a function of Cr thickness [1], an additional short two monolayer oscillation period was found [7,8] exhibiting phase slips [7]. These phase slips are consistent with the same nesting vector which gives rise to the incommensurate spin density wave (ISDW) antiferromagnetism in bulk Cr. Current models for oscillatory exchange coupling [9–12] readily explain the short period oscillation and the phase slips as a result of this nesting vector, independent of the existence of any magnetic long range order (LRO) of the Cr [13], in the same way as for nonmagnetic interlayers. Initial experiments [14,15] yielded contradictory results on the existence of any LRO in Cr interlayers.

The importance of the structure of the Fe/Cr interfaces has been pointed out by many authors [5,7,16]. For example, it was demonstrated that for a given substrate the lateral length scale of the interface fluctuations increases strongly with the growth temperature, drastically modifying the coupling behavior [5,17,18]. In the recent proximity magnetism model [19] for NC coupling, such interface fluctuations and the intrinsic magnetism of AF interlayers such as Cr or Mn were taken into account, yielding a parabolic expression for the exchange energy causing an asymptotic approach to the saturated state as a function of applied field, in contradiction to the usual bilinear-biquadratic [3] exchange coupling formalism. Recent band structure calculations confirm this picture [20]. Although the asymptotic approach has been found in Fe/Cr(001) [18] and FeCo/Mn [21], no direct information on the magnetic structure of the interlayers in such NC coupled superlattices exists.

Here we present high angle neutron scattering data, giving access to the magnetic structure of the Cr interlayers in Fe/Cr(001) superlattices. The results are correlated with polarized neutron reflectometry (PNR) and magneto-optic Kerr effect (MOKE) data on the coupling of the Fe layers. For the smallest Cr thickness investigated, strong NC exchange coupling between the Fe layers occurs as soon as a frustrated, commensurate structure of AF Cr spirals forms below its Néel temperature. This highlights the essential contribution of Cr order to the coupling. Thus, the correlation between Cr order and coupling is exactly opposite to the one reported previously [15,22,23] for larger Cr thicknesses, where an ISDW forms. For this regime we confirm the predicted [24], previously overlooked transition from an incommensurate to a commensurate SDW with increasing temperature.

The samples were grown in a molecular beam epitaxy (MBE) system at 300 °C at a pressure $\leq 10^{-10}$ mbar using growth rates of 0.16 Å/s for Cr and 0.2 Å/s for Fe on a Cr/Nb buffer system on Al_2O_3 $(1\bar{1}02)$ substrates [25]. To maximize the amount of Cr, large 5×5 cm^2 substrates were used and up to 200 Fe/Cr bilayers were grown. Reflection high energy electron diffraction performed during growth indicated a smooth growth front with steps and a smoothing during growth. High angle x-ray data with sharp superlattice peaks up to third order are proof of a coherent superlattice structure. Energy dispersive x-ray (EDX) analysis yielded the relative Fe and Cr contents which, combined with the measured superlattice period, provided the layer thicknesses. X-ray scattering and EDX spectra taken from the center and near the edges of the samples confirmed a perfect lateral homogeneity obtained by continuous rotation of the sample during growth.

High angle neutron measurements were performed at NIST on the SPINS spectrometer. Bulk Cr is AF below its Néel temperature $T_{N,\mathrm{ISDW}} = 311$ K, exhibiting an

 0031-9007/97/79(24)/4914(4)$10.00

ISDW. Depending on polarization (longitudinal or transverse) and propagation, the ISDW causes a *double* peak structure around certain {001} positions [6]. A commensurate AF order causes *single* peaks at the {001} positions. Our findings are summarized in Fig. 1 as a function of Cr interlayer thickness D_{Cr} and temperature for $D_{\mathrm{Fe}} \approx 20$ Å. The insets indicate schematically the observed intensity around (001) with the arrows pointing along the [001] (out of plane) direction. ISDW double peaks were observed for $D_{\mathrm{Cr}} = 80$ Å at low temperatures, indicating a transverse ISDW propagating along [001], i.e., with the moments in the film plane [6,26]. Between about 175 and 310 K we observe a gradual transition (marked T in Fig. 1) from incommensurate (I) to commensurate AF order (C). Furthermore, we find a Néel temperature $T_{N,\mathrm{COM}} \approx 500$ K of this C phase, above which the Cr becomes paramagnetic (P). Naively, the I to C transition could be correlated with the increase of the ISDW period with temperature, as it occurs in bulk: For a given D_{Cr}, a single ISDW period cannot form above a certain temperature and the LRO becomes C. For thinner $D_{\mathrm{Cr}} \approx 42$ Å we find only strong, modulated C peaks which again vanish at $T_{N,\mathrm{COM}} \approx 500$ K. Thus, below a $D_{\mathrm{Cr,min}}$ the ISDW cannot form even for the lowest temperature measured. $T_{N,\mathrm{COM}}$ is significantly enhanced with respect to the bulk $T_{N,\mathrm{ISDW}}$. Such high $T_{N,\mathrm{COM}}$ have been observed in strained C Cr in bulk [6]. Our observations are qualitatively consistent with a recent theoretical study [24] of Fe/Cr with ideal interfaces predicting the C to I transitions as a function of D_{Cr} and T observed here. Finally, we point out that we always find strong intensity at or around a (001) reflection below $T_{N,\mathrm{COM}}$. Since neutron scattering is sensitive only to magnetic moment components perpendicular to the scattering vector, this indicates an in-plane orientation of the magnetic moments in the D_{Cr} range discussed here. As we show elsewhere [26], a reorientation occurs for larger D_{Cr}.

Now we focus on the sample $[\mathrm{Cr}_{42}/\mathrm{Fe}_{19}]_{200}$, with the C order below $D_{\mathrm{Cr,min}}$. The subscripts in the brackets designate the layer thicknesses in Å, whereas the one outside gives the number of bilayers. To characterize the magnetic order of the Fe layers we used hysteresis loops measured by MOKE and PNR with polarization analysis as detailed in Ref. [18]. A PNR scan of the sample taken at room temperature [27] near remanence on the reflectometer BT-7 at NIST is shown in the left inset of Fig. 2. The splitting in the $(++)$ and $(--)$ data, together with the existence of a first order peak at about 0.1 Å$^{-1} \approx 2\pi/\Lambda_{\mathrm{SL}}$ in the $(+-)$ and $(-+)$ scattering, indicate a net magnetization in the sample. In addition, half order peaks at about 0.055 Å^{-1} are observed in all cross sections, indicating that the magnetic period $\Lambda_{\mathrm{Fe,NC}}$ is doubled with respect to the chemical superlattice period Λ_{SL}. Since collinear AF order could not yield such a net magnetization, the individual Fe magnetizations must be NC oriented [18], consistent with our MOKE results.

In the main part of Fig. 2 a scan along the out-of-plane $[00l]$ direction through (010) taken from the same sample at 30 K is shown. Clearly, on both sides of the fundamental (010) peak, additional satellites are visible. These are proof for a *modulation* of the C AF structure with a period $\Lambda_{\mathrm{Cr,AF}}$. The separation $\Delta Q = 2\pi/\Lambda_{\mathrm{Cr,AF}}$ between the satellites is the same as the one observed between the first and half-order peaks in the PNR spectrum in the inset. Thus, we find $\Lambda_{\mathrm{Cr,AF}} = \Lambda_{\mathrm{Fe,NC}} = 2\Lambda_{\mathrm{SL}}$. This would result from the coupling between Fe and Cr at each interface being equal: In the right inset of Fig. 2 the Fe magnetizations are shown

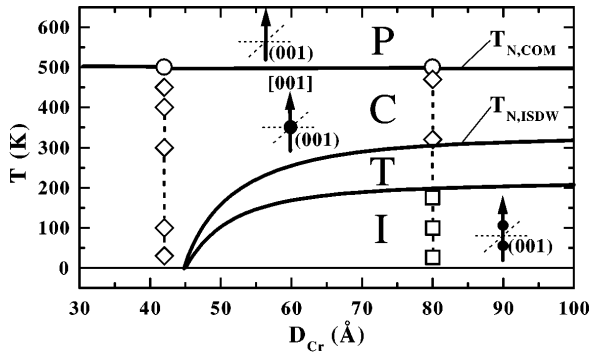

FIG. 1. Phase diagram summarizing the magnetic structure of the Cr interlayers. Diamonds denote commensurate SDW (C), squares denote incommensurate SDW (I), and circles denote paramagnetic (P) regions. T is a transition region. The insets schematically indicate the measured intensity (dots) around (001) with the arrows denoting the [001] scan direction.

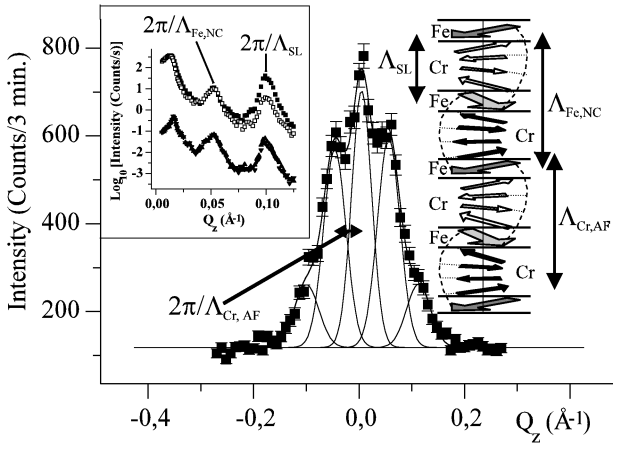

FIG. 2. Left inset: PNR of the sample $[\mathrm{Cr}_{42}/\mathrm{Fe}_{19}]_{200}$ at RT in $B = 14$ G, indicating NC coupling of the Fe layers with $2\Lambda_{\mathrm{SL}} = \Lambda_{\mathrm{Fe,NC}}$. The full squares indicate $(++)$, the empty ones $(--)$ and the up and down triangles $(+-)$ and $(-+)$ scattering. $+$ $(-)$ designate the neutron spin state up (down) before and after the sample, respectively. The $(+-)$ and $(-+)$ data are shifted by 10^{-2}. Main part: High angle l scan through the (010) position at $T = 30$ K for the same sample. Also shown is a fit to the data using five Gaussians separated by $\Delta Q = 2\pi/\Lambda_{\mathrm{Cr,AF}}$. Right inset: schematic of the magnetic structure deduced from the data in the figure fulfilling $\Lambda_{\mathrm{Cr,AF}} = \Lambda_{\mathrm{Fe,NC}} = 2\Lambda_{\mathrm{SL}}$. The empty and filled small arrows indicate an opposing sense of rotation of the Cr moments between the NC coupled Fe layers (large arrows).

as large arrows in a NC structure with $\Lambda_{\mathrm{Fe,NC}} = 2\Lambda_{\mathrm{SL}}$ as found by PNR. The AF Cr moments in between are represented by the smaller arrows (filled and empty for two senses of rotation). The spiral-type modulation of the AF Cr interlayers is the topologically simplest assumption with the boundary condition of AF coupling [28] at *each* Fe/Cr interface. A consequence of this equal coupling is $\Lambda_{\mathrm{Cr,AF}} = \Lambda_{\mathrm{Fe,NC}}$ as observed [29]. The higher order satellites in the data of Fig. 2 indicate rather sharp interfaces of the AF Cr structure.

The coherence length of the magnetic order of the Cr along the growth direction can be determined from scans through (001) along $[00l]$. As shown in Fig. 3, we again observe a multicomponent intensity around the (001) position. The peak can be decomposed into a sharp fundamental reflection and one satellite peak on each side [30]. As in Fig. 2, these satellites are offset with respect to the fundamental reflection by $\Delta Q = 2\pi/\Lambda_{\mathrm{Cr,AF}}$. However, they are much broader. This indicates an out-of-plane coherence length of only about 60 Å for the AF Cr modulation. Thus, we observe coherence of the NC order of the Fe layers over many bilayers (from the PNR data) and of the *C* AF structure of the Cr (from the sharp central peak in Fig. 3). On the other hand, we find a short coherence of the AF Cr *modulation*. Consequently, the schematic in the inset of Fig. 2 is idealized.

In the following, we consider disorder. In the inset of Fig. 3 the effect of Cr interlayer thicknesses fluctuating by one monolayer is shown schematically. Comparing the left and right parts of the figure, we find that the *sense of rotation* of the partial Cr spirals changes upon varying the number of Cr monolayers by one within the *same* Cr layer. This is a consequence of the equal coupling at each Fe/Cr interface and was demonstrated by

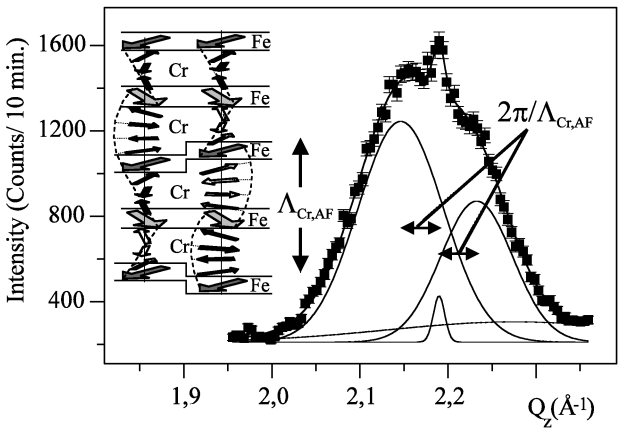

FIG. 3. High angle l scan through the (001) position at $T = 30$ K for the same sample as in Fig. 2. Also shown is a fit to the data using three Gaussians which again are separated by $\Delta Q = 2\pi/\Lambda_{\mathrm{Cr,AF}}$. Inset: Modification of the model in Fig. 2 by inserting a vertically uncorrelated lateral Cr interlayer thickness fluctuation which reduces the coherence explaining the broad satellites. The empty and filled small arrows again indicate opposing senses of rotation.

Slonczewski [19] in his proximity magnetism model for NC coupling. Comparison of the schematics in Figs. 2 and 3 shows that this arbitrary variation of the sense of rotation strongly reduces the coherence of the *modulation* of the AF Cr in the out-of-plane (l) direction. Structure factor calculations confirm the model structure depicted in Fig. 3. Specifically, these calculations also reproduce the line shape in the main part of Fig. 2, confirming the insensitivity of such a scan to the vertical disorder. Furthermore, the small intensity of the central peak in Fig. 3 is explained as a destructive interference due to fluctuating Fe thicknesses. The lateral disorder depicted in the model structure of Fig. 3 is fully confirmed, e.g., by recent diffuse x-ray scattering data from similarly prepared Fe/Cr superlattices [18]. Also it is obvious that the in-plane magnetic structure must be limited in coherence as well due to the lateral fluctuation. From the width of a scan along the in-plane $[0k0]$ direction through (010), we obtain a coherence length of about $L_C^{\parallel} = 150$ Å. The Cr spiral structure, which we postulated from topology arguments, can be tested with polarized neutrons and polarization analysis. Repeating the scan of Fig. 3 we find the same intensity within statistics in all four cross sections consistent with a spiral distribution of the Cr moments. More details will be discussed elsewhere. Finally, we again point out that the observation of strong (001) intensity requires the in-plane orientation of the Cr moments assumed so far.

Thus, we have demonstrated that all aspects of the magnetic structure postulated in the proximity magnetism model [19] are actually observed. In the model, the occurrence of NC coupling is explained by the opposing torque which laterally coexisting partial spirals apply to the Fe layers. Since the Fe layers can neither couple AF (even number of Cr layers) or FM (uneven number of Cr layers) the system compromises on a NC orientation. Slonczewski [19] also provides an upper limit on the lateral length scale $L^{\parallel}$ of D_{Cr} fluctuations, above which the magnetic exchange stiffness of the Fe becomes too weak to prevent the formation of AF- and FM-coupled domains. This value is consistent with the measured $L_C^{\parallel}$ which is directly connected to $L^{\parallel}$.

So far we have correlated NC coupling between the Fe layers with a specific LRO in the Cr interlayers. Finally, we study the effect on the coupling between the Fe layers when the Cr order vanishes at $T_{N,\mathrm{COM}}$. In Fig. 4 the temperature dependence of the (001) peak intensity is shown for the same sample. Clearly, the LRO in the Cr interlayers vanishes at about 500 K. In the insets we show hysteresis loops measured by MOKE along an easy axis of the in-plane anisotropy at and below $T_{N,\mathrm{COM}}$. Below $T_{N,\mathrm{COM}}$, the sample is not saturated at 2 kOe, indicating strong exchange coupling. In passing, we note that equivalent hysteresis loops measured up to 10 kOe indicate the asymptotic approach to saturation expected for the proximity magnetism model [18,21]. At $T_{N,\mathrm{COM}}$ we observe square hysteresis loops, indicating parallel

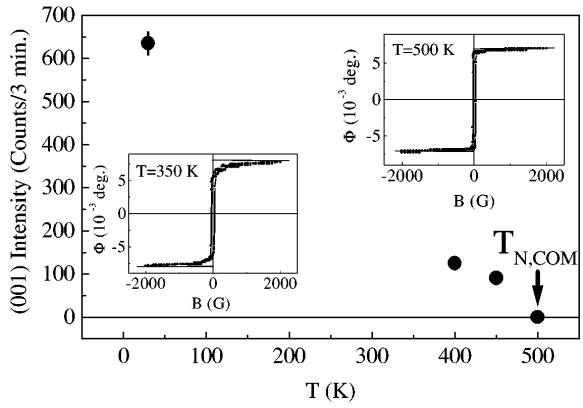

FIG. 4. Neutron (001) intensity as a function of temperature indicating $T_{N,\mathrm{COM}} \approx 500$ K. In the insets typical MOKE hysteresis loops measured below and at $T_{N,\mathrm{COM}}$ are shown. At $T_{N,\mathrm{COM}}$ the NC coupling between the Fe layers vanishes, consistent with PNR results.

alignment of the Fe layers. Consistently, the PNR half-order peak observed below $T_{N,\mathrm{COM}}$ vanishes above $T_{N,\mathrm{COM}}$ in a 60 G field. Thus, the strong NC exchange coupling observed below $T_{N,\mathrm{COM}}$ vanishes with the Cr LRO.

Finally, we discuss our results in the framework of other available data. Meersschaut *et al.* [14] found a longitudinal ISDW with the moments oriented *out of the film plane* for D_{Cr} above 75 Å and measured Cr to be nonmagnetic for thicknesses below 60 Å by perturbed angular correlation spectroscopy. Here we clearly observe *C* LRO down to smaller D_{Cr}, where no ISDW forms. Furthermore, in the whole D_{Cr} range discussed here, the Cr moments are predominantly *in the film plane*. Our results are confirmed by Fullerton *et al.* [15]. The solid lines separating the *C* and *I* regions in Fig. 1 were chosen such that the Cr thickness dependent $T_{N,\mathrm{ISDW}}$ reported in Ref. [15] essentially lies in our transition region (T) from *I* to *C* order. However, in Ref. [15] a paramagnetic phase above $T_{N,\mathrm{ISDW}}$ is reported, whereas here we find proof for *C* AF order in this regime, qualitatively consistent with theoretical predictions [24].

In conclusion, we find strong NC coupling only *below* the ordering temperature of a frustrated *C* AF spiral structure in the Cr layers. So far, spiral magnetic structures have only been observed in the rare earths [31]. The correlation between coupling and Cr order reported here is exactly opposite to the results for larger thicknesses in the *I* phase. In this case the *absence* of coupling has been correlated with the occurrence of Cr LRO [22,23]. Thus, for this important model system we have clarified the essential contribution of Cr order in the thickness regime, where all important aspects of exchange coupling were discovered. Furthermore, we find an *I* to *C* phase transition for large Cr thicknesses, as predicted by theory.

We gratefully acknowledge discussions with H. Zabel and J. Borchers. We thank V. Nunez and S. H. Lee for their support with SPINS, and I. Zoller for spending nights with sample preparation. Financial support was provided by NATO (CRG 901064), as well as the German BMBF (03-ZA4BC2 -3) and DFG via SFB 166.

[1] P. Grünberg *et al.*, Phys. Rev. Lett. **57**, 2442 (1986); S. S. P. Parkin, N. More, and K. P. Roche, Phys. Rev. Lett. **64**, 2304 (1990); S. Demokritov, J. A. Wolf, and P. Grünberg, Europhys. Lett. **15**, 881 (1991).
[2] M. N. Baibich *et al.*, Phys. Rev. Lett. **61**, 2472 (1988); G. Binasch, *et al.*, Phys. Rev. B **39**, 4828 (1989).
[3] M. Rührig *et al.*, Phys. Status Solidi (a) **125**, 635 (1991).
[4] B. Heinrich *et al.*, Phys. Rev. B **44**, 9348 (1991).
[5] B. Heinrich and J. F. Cochran, Adv. Phys. **42**, 523 (1993).
[6] E. Fawcett, Rev. Mod. Phys. **60**, 209 (1988).
[7] J. Unguris, R. J. Cellotta, and D. T. Pierce, Phys. Rev. Lett. **67**, 140 (1991).
[8] S. T. Purcell *et al.*, Phys. Rev. Lett. **67**, 903 (1991).
[9] Y. Wang, P. M. Levy, and J. L. Fry, Phys. Rev. Lett. **65**, 2732 (1990).
[10] P. Bruno and C. Chappert, Phys. Rev. Lett. **67**, 1602 (1991).
[11] D. M. Edwards *et al.*, Phys. Rev. Lett. **67**, 493 (1991).
[12] M. D. Stiles, Phys. Rev. B **48**, 7238 (1993).
[13] M. van Schilfgaarde and F. Herman, Phys. Rev. Lett. **71**, 1923 (1993); D. Stoeffler and F. Gautier, Phys. Rev. B **44**, 10 389 (1991).
[14] J. Meersschaut *et al.*, Phys. Rev. Lett. **75**, 1638 (1995).
[15] E. E. Fullerton, S. D. Bader, and J. L. Robertson, Phys. Rev. Lett. **77**, 1382 (1996).
[16] J. A. Wolf *et al.*, J. Magn. Magn. Mater. **121**, 253 (1993).
[17] D. T. Pierce *et al.*, Phys Rev. B **49**, 14 564 (1994).
[18] A. Schreyer *et al.*, Europhysics Lett. **32**, 595 (1995); Phys. Rev. B **52**, 16066 (1995).
[19] J. C. Slonczewski, J. Magn. Magn. Mater. **150**, 13 (1995).
[20] M. Freyss, D. Stoeffler, and H. Dreyssé, Phys. Rev. B **54**, R12 677 (1996).
[21] M. E. Filipkowski *et al.*, Phys. Rev. Lett. **75**, 1847 (1995).
[22] E. E. Fullerton *et al.*, Phys. Rev. Lett. **75**, 330 (1995).
[23] J. F. Ankner *et al.*, J. Appl. Phys. **81**, 3765 (1997).
[24] Z. P. Shi and R. S. Fishman, Phys. Rev. Lett. **78**, 1351 (1997).
[25] For details, see S. Di Nunzio, K. Theiss-Bröhl and H. Zabel, Thin Solid Films **279**, 180 (1996); I. Zoller *et al.*, Phys. Rev. B (to be published).
[26] P. Sonntag *et al.*, J. Magn. Magn. Mater. (to be published).
[27] Temperature dependent PNR measurements confirm that the spectra remain essantially unchanged between 30 K and RT in case of field or zero-field cooling.
[28] See, e.g., F. U. Hillebrecht *et al.*, Europhys. Lett. **19**, 711 (1992).
[29] This would also result either for FM coupling at *all* Fe/Cr interfaces or for AF coupling at *all* top (bottom) and FM coupling at *all* bottom (top) interfaces of each Cr layer, respectively.
[30] As opposed to Fig. 2, the fit yields negligible higher order satellite intensities.
[31] See, e.g., M. B. Salomon *et al.*, Phys. Rev. Lett. **56**, 259 (1986), and references therein.